

Two-Dimensional Mapping of Copper and Zinc in Liver Sections by Laser Ablation–Inductively Coupled Plasma Mass Spectrometry

ANDREW KINDNESS,^{1,2} CHANDRA N. SEKARAN,¹ and JÖRG FELDMANN^{1*}

Background: Metals are not homogeneously distributed in organ tissues. Although most mapping techniques, such as histologic staining methods, have been developed for element imaging on a subcellular level, many suffer from either low precision or poor detection limits. Therefore, small variations in elemental distribution cannot be identified. We developed a method for two-dimensional mapping of trace elements to identify the influence of metabolic zonation by the liver on trace element distribution.

Methods: A prepared homogeneous Certified Reference Material (CRM; LGC 7112, pig liver) was used to characterize the laser ablation–inductively coupled plasma time-of-flight mass spectrometry (LA-ICP-MS) in terms of precision. Different isotopes for copper and zinc were monitored, and the use of carbon as an internal standard was investigated to correct for differences in ablation efficiency to identify the most precise mapping technique for liver samples.

Results: For the homogeneous CRM, the reproducibility of the copper and zinc signals was ~3–24% depending on spot size and number of pulses. When carbon was used as an internal standard, the reproducibility was improved significantly. Line scan signals over a length of 1.5 mm were more precise [relative SD (RSD), 1.6–6.1% for copper (⁶³Cu, ⁶⁵Cu) and zinc (⁶⁴Zn, ⁶⁶Zn) depending on the spot size, the scanning speed, and the element]. Thin section of sheep liver achieved precisions of 27–59% (raster scan) and 9–47% (line scan) RSD for copper, whereas the precision for zinc was significantly better: 8–18% (raster scan) and 4–21% (line scan) RSD. Long line scans and two-dimensional element

maps of the thin sections revealed the zonation of copper in sheep liver containing extremely low copper concentrations.

Conclusion: Elemental mapping of trace elements generated by LA-ICP-MS can be very precise so that small changes in the elemental concentration in the tissue can be detected and nonuniform spatial distribution of the elements in tissues can be established.

© 2003 American Association for Clinical Chemistry

Biochemists and toxicologists gain information about the concentrations of trace and ultratrace metals in different tissues by use of large amounts of homogenized tissue, which is digested so that a total metal analysis can be performed. This assumes that every cell is the same. In biological and clinical applications, however, it is often desirable to gain knowledge about the distribution of a trace element in a soft tissue. Traditionally, pathologists have used staining methods for the different elements of interest. These methods have disadvantages: they are often not sensitive enough to detect trace and ultratrace concentrations of elements, or the chemicals used for staining introduce impurities (1). Although these methods are element specific, this is a disadvantage if more than one element has to be mapped in the tissue. In addition, some of the chemical reactions are very metal species specific. For example, complexing agents must compete with cysteine-rich proteins (metallothioneins) to bind the metal. Thus, staining methods such as the rhodamine method for copper can identify free copper but not the copper bound in copper proteins (2). Other methods, such as scanning nuclear microprobes (1), microPIXE (3), secondary ion mass spectrometry (4, 5), laser microprobe mass analysis (6), energy-dispersive x-ray analysis (7–9), and electron probe x-ray microanalysis (10), suffer from either low precision or poor detection limits. Laser microprobe mass analysis, however, is an ideal technique for the determination of trace element distribution in biological samples. It is a rather sensitive tool, with detection limits in the upper ppm range (1–100

¹ Environmental Analytical Chemistry, University of Aberdeen, Old Aberdeen AB24 3UE, Scotland, UK.

² School of Pure & Applied Chemistry, University of Natal, Durban, South Africa 4001.

*Author for correspondence. E-mail j.feldmann@abdn.ac.uk.

Received May 15, 2003; accepted August 27, 2003.

Previously published online at DOI: 10.1373/clinchem.2003.022046

Table 1. Optimized conditions for LA-ICP-TOF MS using the cryogenically cooled ablation cell for the analysis of soft tissue.

Conditions	Renaissance (LECO)	LSX 200 Plus (CETAC)
ICP-TOF-MS		
Forward power (40.68 MHz)	1400 W	
Plasma flow	14.2 L/min	
Auxiliary flow	0.67 L/min	
Carrier gas (Ar) flow	1.12 L/min	
Integration time	0.5 s	
Measured masses	^{12}C , ^{13}C , ^{64}Zn , ^{66}Zn , ^{68}Zn , ^{63}Cu , ^{65}Cu , and background m/z 220, m/z 5	
Internal standard	^{13}C or ^{12}C (partly deflected)	
Deflected masses	m/z 12, 23, 36–55, 80	
Detector (pulse counting/analog)	–2750 V	
LA		
Laser		Nd-YAG
Wavelength		266 nm
Laser energy density		12.2 J/cm ² (100% power)
Focus		Sample surface
No. of pulses/spot		1–20
Pulse frequency		10 Hz
Spot size		10–250 μm
Cryogenic cell temperature		–80 °C

$\mu\text{g/g}$). However, because the ionization of elements is strongly dependent on the matrix and therefore rather difficult to calibrate, this technique can be considered only as a qualitative method. Furthermore, the thin sections should not be thicker than 2 μm , which makes sample preparation rather difficult.

Laser ablation (LA)³ methods have been used extensively for the mapping of elements and organic compounds in soft tissue. Recent developments in matrix-assisted laser desorption-ionization time-of-flight mass spectrometry allow a spatial resolution of 30 μm for the direct mapping of compounds in the mass range between 1 and 50 kDa in tissue sections (4, 11). However, when a LA system is coupled to an inductively coupled plasma mass spectrometer (ICP-MS), the ablated material is fully ionized in the argon plasma and the elements are detected by an element-specific detector (12). Only a few studies, however, have used this method for soft tissues (13, 14). In our previous study we used LA coupled to inductively coupled plasma time-of-flight mass spectrometry (ICP-TOF-MS) for the quantification of trace elements in soft tissues. Here we report a study on the use of this technique to map trace elements in homogenized liver and in thin sections of sheep liver and show that copper shows zonations whereas zinc is reasonably constant.

Materials and Methods

INSTRUMENT SET-UP

We used a commercially available Nd-YAG laser with frequency quadrupling to attain 266 nm (CETAC LSX-200

Plus and DigiLaz operating software) coupled to an ICP-TOF-MS (Renaissance; LECO). A cryogenically cooled ablation cell of similar size (volume, 60 mL) replaced the commercial ablation chamber. The temperature was controlled from –20 to –100 °C with a variance of ± 3 °C within the ablation cell. The pulse duration was 5 ns, and the maximum pulse frequency was 20 Hz. The energy density was constant at a maximum of 12 J/m³ with a focal spot size between 10 and 250 μm . More details are given in a previous publication (13). The ICP-MS was tuned on m/z 59 for cobalt, m/z 139 for lanthanum, and m/z 232 for thorium by the continuous ablation of a reference glass sample, SRM NIST 612. [The stability of the laser and the ICP-MS give a precision of better than 4% relative SD (RSD) for an 8-min continuous line scan of 25 $\mu\text{m/s}$ and a frequency of 20 Hz for cobalt (35.5 mg/kg), lanthanum (36 mg/kg) and thorium (15.7 mg/kg).] The plasma conditions for the frozen tissue samples (liver) were optimized on m/z 63 for copper (^{63}Cu) and m/z 66 for zinc (^{66}Zn). The optimized plasma conditions are given in Table 1. Some modifications, described in the text, were used for individual experiments.

SAMPLES AND STANDARDS

Two different samples of sheep liver were used. The first was a liver sample from a wild North Ronaldsay sheep. These sheep live on the shores of the small Scottish island of North Ronaldsay. Although their main diet includes different types of seaweed (15) containing relatively high amounts of copper, this copper is not bioavailable; hence, they have a low copper concentrations in the liver (NR liver) (16). The second was a commercially available lamb liver from New Zealand (NZ liver), which was used as an

³Nonstandard abbreviations: LA, laser ablation; ICP-MS, inductively coupled plasma mass spectrometry; TOF, time of flight; RSD, relative SD; NR, North Ronaldsay; NZ, New Zealand; and CRM, Certified Reference Material.

example of the typical copper concentrations in sheep liver. The frozen samples were carefully sliced to $\sim 35\text{-}\mu\text{m}$ thickness with a microtome at $-25\text{ }^\circ\text{C}$ (OTF-cryostat; Bright Instruments). It is essential to produce a flat surface over the entire tissue to reproduce the same ablation conditions for the entire tissue. As a standard reference material, we used a certified pig liver paste (LGC 7112; certified by LGC, Teddington, UK). This is a homogenized paste and contains water ($\sim 70\%$). The certified reference material (CRM) was pressed between two pieces of glass with a 2-mm spacer and then frozen to generate a dense, homogeneous tissue-like sample with a smooth surface.

BULK ANALYSIS OF SAMPLES BY LA-ICP-MS

The use of the tissue-like CRM liver paste (LGC 7112) for the quantification has been demonstrated in a previous study (13). The NR liver section and the NZ liver samples were quantified with use of LGC 7112 in a standard, bracketing one-point calibration technique. We made 1-mm-thick frozen section of the sheep liver samples and placed them in the ablation chamber together with the tissue-like CRM LGC 7112. The samples were kept at $-80\text{ }^\circ\text{C}$ and subsequently ablated on five discrete spots. The laser was operated at each spot for 1 s with a pulse frequency of 10 Hz. The energy density on the $250\text{-}\mu\text{m}$ spot was 12.2 J/cm^3 . The carbon signal (^{12}C or ^{13}C) was used as an internal standard because the carbon content of the dry mass of liver tissues is reasonably constant. This allows correction for any differences in the laser fluctuation, surface roughness, and a change in the absorption coefficient of the tissue. The copper to carbon ratio ($^{63}\text{Cu}/^{12}\text{C}$) and the zinc to carbon ratio ($^{66}\text{Zn}/^{12}\text{C}$) of the CRM was used for the one-point calibration.

MAPPING EXPERIMENTS

Two different mapping methods were tested: the raster scan and the line scan. The raster scan was defined as 10 discrete single spots in a line with a distance of $300\text{ }\mu\text{m}$ between the spots; the spot size and the number of laser pulses used were varied. The second method is the line scan. Here the laser was always operated with the same pulse frequency of 10 Hz, but the sample was moved along a well-defined line of $\sim 1500\text{ }\mu\text{m}$ throughout the ablation process, creating a trench in the sample instead of numerous discrete spots. For this method the scan speed and the spot size were varied. The scan speed defines the depth of the trench, whereas the spot size defines the width.

The analog signal (in mV) and the pulse-counting signal (in cps) from each m/z channel of the ICP-MS were blank-subtracted, and the peak areas for the individual spots were determined by trapezium integration. The blank was defined by the signal produced without the laser in operation. For each mapping method, the reproducibilities of the copper, zinc (as examples of trace elements in the liver), and carbon (as the matrix element) signals were calculated, and the use of carbon as an

Table 2. Reproducibility and intensity of copper, zinc, and carbon of the raster scans in CRM pig liver LGC 7112.^a

Spot size, μm	No. of pulses	RSD, %										Intensity ^b		
		^{63}Cu	^{65}Cu	$^{63}\text{Cu}/^{65}\text{Cu}$	$^{63}\text{Cu}/^{12}\text{C}$	$^{65}\text{Cu}/^{12}\text{C}$	^{64}Zn	^{66}Zn	$^{64}\text{Zn}/^{66}\text{Zn}$	$^{64}\text{Zn}/^{12}\text{C}$	$^{66}\text{Zn}/^{12}\text{C}$	^{12}C	^{63}Cu	^{64}Zn
100	20	19	19	1.8	14	14	23	23	2.9	18	18	10.1	7858	44.9
	10	15	15	1.8	11	12	12	12	2.3	10	9.7	5.57	4679	25.8
	5	16	14	2.9	7.1	5.3	12	8.9	3.6	7.4	7.9	3.30	3273	13.1
	2	17	11	2.7	5.2	7.5	13	12	4.1	11	10	1.19	1480	5.9
	1	15	19	7.8	11	9.3	22	24	11	15	18	0.94	799	3.0
200	20	16	16	0.73	9.1	9.3	16	14	2.5	10	9.9	42.1	4.54 ^c	194
	10	12	12	2.9	7.8	7.5	6.9	8.3	2.2	5.2	6.9	25.1	15 440	104
	5	6.6	9.9	1.1	8.6	9.9	8.1	9.5	1.8	5.1	6.2	13.6	10 945	54.5
	2	13	14	2.5	4.9	3.2	10	11	2.2	9.6	9.4	5.97	5743	24.6
	1	8.2	8.6	3.3	9.6	8.6	10	11	2.1	9.6	10	3.05	2941	12.3

^a The raster scan conditions were spot sizes of 100 and 200 μm , 10 points with distance of 300 μm , 6.5 ml, and 10 Hz frequency. The number of pulses and the spot sizes were altered.

^b Intensities are in mV for ^{63}Cu and ^{12}C , and in cps for ^{64}Zn .

^c Intensity of zinc reached nonlinearity of the detector in pulse-counting mode; this intensity was therefore measured in mV.

internal standard was studied. The reproducibility was calculated based either on 10 individual peak areas or on peak-area ratios, when the internal standard carbon was used. A similar procedure was used for identification of the variability of a line scan; however, instead of using the peak area of 10 spots, we used every measuring point for the 1500- μm scan.

All of these methods were also performed on the microtomed thin section of a NR sheep liver to identify small variations in the copper concentration of a liver sample with low copper concentrations.

Results and Discussion

BULK ANALYSIS

The zinc concentrations in both liver samples were similar, 42 mg/kg for NZ liver and 50 (4) mg/kg [mean (SD)] for NR liver, whereas the copper concentrations were very different [7 mg/kg for NZ liver and 1 (4) mg/kg for NR liver]. The copper concentration in both samples was very low, with the concentration in the NR sheep liver being extremely low. It is well known that if high copper concentrations are found in the liver, they are not uniformly distributed (17, 18). The low copper concentrations found in these samples make them ideal for studying the performance of the new mapping technique for trace elements to determine whether zonation of copper at low concentrations can be identified.

MAPPING OF THE HOMOGENEOUS CRM SAMPLES

The intensities and variability of the copper, zinc, and carbon signals using the different raster scans are shown in Table 2, whereas the data for the line scan are shown Table 3.

The homogeneous pig liver (LGC 7112) showed a remarkably stable constant signal for ^{12}C , which varied only between 2% and 6% RSD for the line scan, whereas the raster scan of a similar length gave a RSD of ~4–15%. The line scan generated much more data than the raster line, which explains the higher precision of the line scan. The variability of the line scan is not significantly different from that of the used glass sample (NIST 612) for which RSD values of ~4% have been achieved.

The RSD values for zinc and copper were slightly but not significantly higher for both methods. The different raster scans showed RSDs of 8–19% for copper (^{63}Cu and ^{65}Cu) and 7–23% for zinc (^{64}Zn and ^{66}Zn), whereas again the line scans showed lower RSDs for copper (3–6%) and for zinc (4–8%).

Because the reproducibilities of the trace elements and the matrix element are similar, carbon was tested as an internal standard. The use of carbon as internal standard improved the precision for the CRM pig liver significantly. For the raster scan, RSDs of 3–14% for $^{63}\text{Cu}/^{12}\text{C}$ and $^{65}\text{Cu}/^{12}\text{C}$ instead of 8–19% for ^{63}Cu and ^{65}Cu , and 5–18% for $^{64}\text{Zn}/^{12}\text{C}$ and $^{66}\text{Zn}/^{12}\text{C}$ compared with 7–23% for ^{64}Zn and ^{66}Zn were achieved, whereas the line scan was again significantly more precise with RSDs of 2–3%

Table 3. Reproducibility and intensities of copper, zinc, and carbon in a 1500- μm line scan of CRM pig liver LGC 7112.^a

Spot size, μm	Scan speed, $\mu\text{m}/\text{s}$	RSD, %										Intensity ^b			
		^{63}Cu	^{65}Cu	$^{63}\text{Cu}/^{12}\text{C}$	$^{65}\text{Cu}/^{12}\text{C}$	$^{63}\text{Cu}/^{65}\text{Cu}$	^{64}Zn	^{66}Zn	$^{64}\text{Zn}/^{12}\text{C}$	$^{66}\text{Zn}/^{12}\text{C}$	$^{64}\text{Zn}/^{66}\text{Zn}$	^{12}C	^{63}Cu	^{64}Zn	^{12}C
50	25	4.9	5.2	3.2	3.2	0.98	7.7	7.6	5.4	5.2	2.4	3.7	5.6	4398	36.1
	50	3.3	3.5	2.9	2.8	0.66	3.6	3.6	3.6	3.9	2.0	2.5	6.5	5172	39.0
100	100	3.8	4.3	1.9	2.3	1.2	4.6	4.6	2.2	2.2	1.4	3.7	7.0	5381	40.0
	25	5.5	5.6	3.0	3.0	0.67	3.7	4.3	3.6	4.0	1.0	3.9	23	14 259	108
100	50 ^c	18	18	6.1	6.0	0.64	12	13	2.8	2.5	1.6	14	22	13 942	107
	100	2.8	3.0	2.1	2.1	0.41	4.6	5.2	1.9	1.6	0.88	5.8	25	14 975	113

^a The scanning conditions were 6.5 mJ of energy at a pulse frequency of 10 Hz. The spot size and the scan speed were altered.

^b Intensities are in mV for ^{63}Cu and ^{12}C , and in cps for ^{64}Zn .

^c This scan suffers from problems during the ablation process, which can be cancelled out by use of ^{12}C as internal standard.

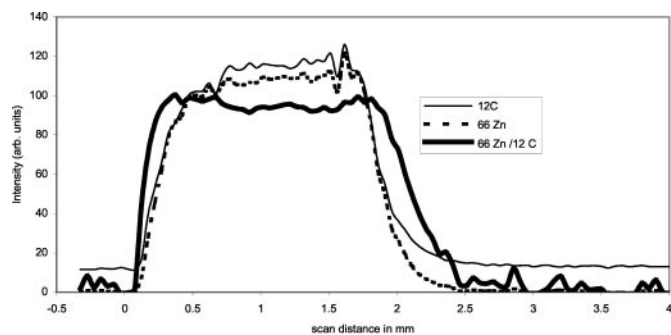


Fig. 1. Line scan of a homogeneous sample (CRM LGC 7112, pig liver) illustrates the use of carbon as internal standard.

Spot size, 100 μm ; scanning conditions, 10 Hz, 6.5 mJ, and 25 $\mu\text{m/s}$. The RSDs for normalized scan signals differed for the different elements: 1.4% for ^{12}C ; 1.3% for ^{64}Zn ; and 2.8% for $^{64}\text{Zn}/^{12}\text{C}$. *arb.*, arbitrary.

or 2–5% for $^{63}\text{Cu}/^{12}\text{C}$ and $^{65}\text{Cu}/^{12}\text{C}$ or $^{64}\text{Zn}/^{12}\text{C}$ and $^{66}\text{Zn}/^{12}\text{C}$, respectively. Fig. 1 illustrates how signal fluctuation during the ablation can be corrected by use of carbon as an internal standard. Although the element carbon ratios ($^{63}\text{Cu}/^{12}\text{C}$ or $^{64}\text{Zn}/^{12}\text{C}$) improved the precision of the element signals, they were still significantly higher than the element ratios ($^{63}\text{Cu}/^{65}\text{Cu}$ and $^{64}\text{Zn}/^{66}\text{Zn}$). Depending on spot size and speed, RSDs of 0.4–1.1% for copper and 0.9–2.5% for zinc were achieved with a line scan, whereas with a raster scan the RSDs were significantly higher (0.7–7.8% for copper; 1.8–11% for zinc). This is also illustrated in Fig. 2. Overall these values are encouraging for the mapping of elements in real tissues because small variations of $\pm 10\%$ in the concentration of trace elements can be identified by both methods with the different conditions.

By analyzing the data in more detail, we can identify the optimal scanning conditions to see small changes in the concentration of the element in the tissue sample. For line scans, high scan speeds, such as 100 $\mu\text{m/s}$, produced a lower RSD for the CRM. An explanation for this effect might be that during LA the surface of the sample is modified not only at the ablated spot but also on the peripheral zones as a result of redeposition of ablated

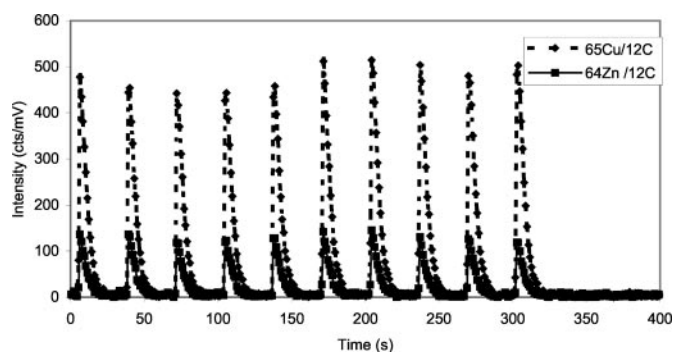


Fig. 2. Raster scan of CRM pig liver LGC 7112 ($^{65}\text{Cu}/^{12}\text{C}$ and $^{64}\text{Zn}/^{12}\text{C}$).

RSDs for the isotope ratios are 2.9% for $^{63}/^{65}\text{Cu}$, 5.3% for $^{65}\text{Cu}/^{12}\text{C}$, and 7.4% for $^{64}\text{Zn}/^{12}\text{C}$. *cts*, counts per second.

material and thermal modification, such as graphitization. With a slow scan speed and a small diameter, the sample surface is more affected by the previous laser pulses. The surface is rougher, and consequently the fluency of the laser is not homogeneously distributed on the sample, which increases the reproducibility of the signal (19). This effect seems to be limited when a faster scan speed and a larger spot size is used. On the other hand, faster scans would produce fewer data points and therefore would suffer from a lower reproducibility. However, because of the combination of speed in relation to the frequency of the laser and the sampling rate of the ICP-MS, material from a larger area is measured at the same time. This mixing effect will smooth the data, which would be desirable for bulk analysis but not for the identification of uneven spatial distribution of metals. The spot size increases the amount of ablated material produced; hence it increases the resulting intensity and consequently improves the RSD. This effect was also seen when the raster scan was used. When discrete spots were used, however, it seemed that the RSDs of the Cu/C and Zn/C ratios for the CRM were strongly dependent on the number of pulses. As expected, the precision increased with increasing number of pulses, but with higher numbers of pulses per spot (>10 pulses) the RSDs again increased. The deeper crater created by more than 10 pulses makes it more likely that the plasma generated on the surface of the sample during the ablation process introduces element fractionation by influencing the transport phenomenon of the ablated material into the plasma of the ICP-MS.

MAPPING OF THE THIN NR SHEEP LIVER SECTIONS

The intensities and variability of the copper, zinc, and carbon signals at the different raster scans are shown in Table 4, whereas the data for the line scans are shown in Table 5. In terms of the relatively nonhomogeneous thin section of the NR lamb liver, the RSDs of the carbon signal (6–26%) were significantly higher than those obtained using the CRM for both raster and line scans (Tables 4 and 5). The relative roughness of the microtomed tissue and the variation of energy absorption by the tissue (because of differences in the color of the liver) may lead to poorer precision. It is apparent that the RSD values for both metals were higher in the thin section of the lamb liver sample compared with the homogeneous tissue-like standard. The variability, in particular for copper (RSD up to 68%), was not reduced significantly by the use of carbon as an internal standard (see Table 4). The signal did not vary randomly, as can be seen for the line scan in Fig. 3 and for the raster scan in Fig. 4. Hence, the high RSDs of the metal/carbon ratios reflect the uneven distribution of the elements in the tissue because the isotope ratios of the elements were significantly lower (mainly 2–6% for $^{63}\text{Cu}/^{65}\text{Cu}$ and 3–9% for $^{64}\text{Zn}/^{66}\text{Zn}$). The slightly higher variability of the element ratios reflects the lower intensities attributable to lower ablated mass of the thin liver section

Table 4. Reproducibility and intensity of copper, zinc, and carbon in the raster scan from a thin section of NR sheep liver.^a

Spot size, μm	No. of pulses	RSD, %					Intensity ^b		
		⁶³ Cu	⁶³ Cu/ ¹² C	⁶⁴ Zn	⁶⁴ Zn/ ¹² C	¹² C	⁶³ Cu	⁶⁴ Zn	¹² C
100	20	34	27	12	12	18	462	515	3.0
	10	68	58	20	15	14	469	544	3.6
	5	57	44	11	18	20	481	478	2.6
	2	31	34	14	14	10	256	312	1.9
	1	63	57	13	13	12	153	209	1.1
200	20	42	50	25	17	23	2167	1865	11.3
	10	67	59	16	14	20	1717	1933	11.8
	5	39	29	11	7.7	11	1518	2028	12.9
	2	46	43	12	9.6	7.9	1013	1103	7.6
	1	36	38	10	9.5	6.0	580	795	4.6

^a The raster scan conditions were a spot size of 100 or 200 μm , 10 points with distance of 300 μm , 6.5 mJ, and 10 Hz frequency. The number of pulses and the spot sizes were altered.

^b Intensities are in mV for ⁶³Cu and ¹²C, and in cps for ⁶⁴Zn.

compared with the pig liver paste. However, it should be noted that the variability of other elements, such as sodium and sulfur, which were been monitored because of their high intensities at m/z 23 and 32, might interfere with the measured isotopes because the mass resolution of our TOF mass spectrometer cannot separate ⁴⁰Ar²³Na⁺ from ⁶³Cu⁺ or ³²S₂⁺/³²SO₂⁺ from ⁶⁴Zn.

The faster scanning speed used here, again like with the homogeneous standard, showed the lowest RSD at the larger spot size, which would confirm that the previous pulses changed the surface of the area that should be ablated.

The number of pulses used for a thin section is limited because the material is usually only 35- μm thick. The sections are not fully penetrated with 5 pulses per spot, but they are with >10 pulses. Hence, only five pulses should be used when thin sections are going to be analyzed.

ZONATION OF LIVER

To map a soft tissue sample, two different modes can be used: raster scans of single shots or linear scans, in which the laser moves with a certain speed (e.g., 25 $\mu\text{m}/\text{s}$) while

ablating. In general, the line scan takes more time, and more material is ablated and transported into the argon plasma. The maximum resolution for the raster scan is 10 μm , whereas for the line scan, the resolution depends on the scan speed and data acquisition. Clearly, however, the resolution is not good enough to determine individual cells or even particular organelles in the different cells, but it is known that the liver is divided into functional units of lobules, which have a diameter of 1 mm (17). On one end, oxygen-rich blood enters the lobules by the artery, whereas the portal veins transport nutrients from the intestine. As a consequence, nutrient and oxygen gradients are generated within the lobules so that different metabolic zones are established. Redox-active and essential trace elements such as copper show an effect of this metabolic zonation when the liver contains high amounts of copper. It has been shown, for example, that rats accumulate copper in the center of the lobules, whereas dogs show an accumulation on the fringe of the lobules, the so-called zone 1 (16). Fig. 3 illustrates the information attained from a line scan of a thin liver section. It is obvious that the zinc concentration does not change over a distance of 1.5 mm, whereas copper shows

Table 5. Reproducibility and intensity of copper, zinc, and carbon of the line scan of a length of 1500 μm from a thin section of NR sheep liver.^a

Spot size, μm	Scan speed, $\mu\text{m}/\text{s}$	RSD, %									Intensity of ¹² C, mV
		⁶³ Cu	⁶⁵ Cu	⁶³ Cu/ ¹² C	⁶³ Cu/ ⁶⁵ Cu	⁶⁴ Zn	⁶⁶ Zn	⁶⁴ Zn/ ¹² C	⁶⁴ Zn/ ⁶⁶ Zn	¹² C	
25	25	48	49	47	3.0	23	23	21	9.4	17	1.7
	50	29	29	22	2.7	18	15	7.6	8.7	13	1.7
	100	19	19	8.5	1.5	10	17	10	8.7	17	1.7
50	25	41	42	32	8.1	15	16	10	7.8	15	1.7
	50	23	26	17	2.8	12	13	4.3	7.3	9.8	2.4
	100	14	32	14	2.6	10	9.0	5.2	4.8	12	4.5
100	25	42	45	26	5.9	26	28	20	8.7	26	2.9
	50	38	33	25	2.9	26	26	7.6	5.0	22	4.0
	100	14	15	8.8	2.0	5.8	6.8	4.9	3.4	6.1	6.3

^a The scanning conditions were 6.5 mJ energy at a pulse frequency of 10 Hz. The spot size and the scan speed were altered.

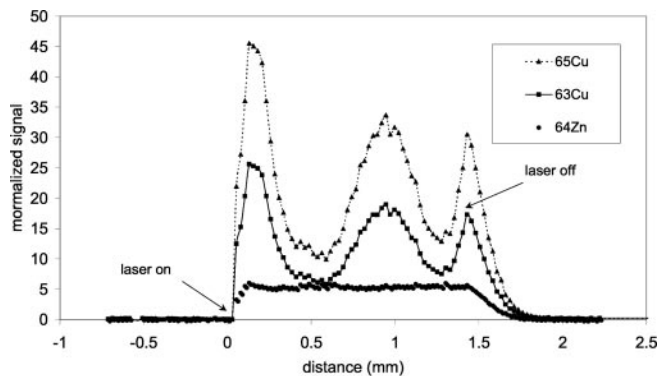


Fig. 3. Line scan of a sheep liver.

Shown are the normalized signals for zinc and both copper isotopes (m/z 63 and 65). Spot size, $100\ \mu\text{m}$; scanning conditions, 10 Hz, 6.5 mJ, and $25\ \mu\text{m/s}$. The RSDs for normalized scan signals are different for the different elements: 44% for ^{63}Cu ; 44% for ^{65}Cu ; and 15% for ^{64}Zn .

zones of accumulation. These zones of accumulations can be determined in a raster scan map (illustrated in Fig. 5). The copper signal fluctuates by more than a factor of 2. The zones of copper accumulation are $\sim 0.3\text{--}0.5\ \text{mm}$ in size, and from one maximum to the next is $\sim 1\ \text{mm}$. A two-dimensional map constructed from a raster scan shows accumulation of copper in certain zones, with areas approximately the same size as identified with the line scan. This is exactly the size of the liver lobules. Those zones may be related to a core of copper accumulated in the center of the lobules. Zones that are supplied with fresh oxygenated blood show different metabolic functions and element concentrations compared with zones in the center of the liver (18). This redox effect would clearly affect the copper more, because copper is more redox active than zinc. The reason for this zonation is not yet clear, but this is the first time that the zonation of copper also has been identified at very low concentrations.

Our aim was to show that these variations can be determined and remain to be explained in the near future. To date this technique has not been available, and the traditional methods were not sensitive enough to reveal

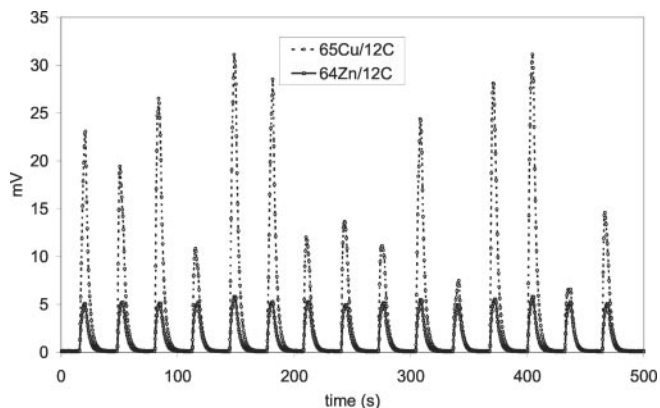


Fig. 4. Raster scan of NZ sheep liver ($^{65}\text{Cu}/^{12}\text{C}$ and $^{64}\text{Zn}/^{12}\text{C}$).

The RSD for the isotope ratio $^{63}/^{65}\text{Cu}$ (peak height) is 0.21%, whereas $^{65}\text{Cu}/^{12}\text{C}$ has a RSD of 32% and $^{64}\text{Zn}/^{12}\text{C}$ has a RSD of 5.8%.

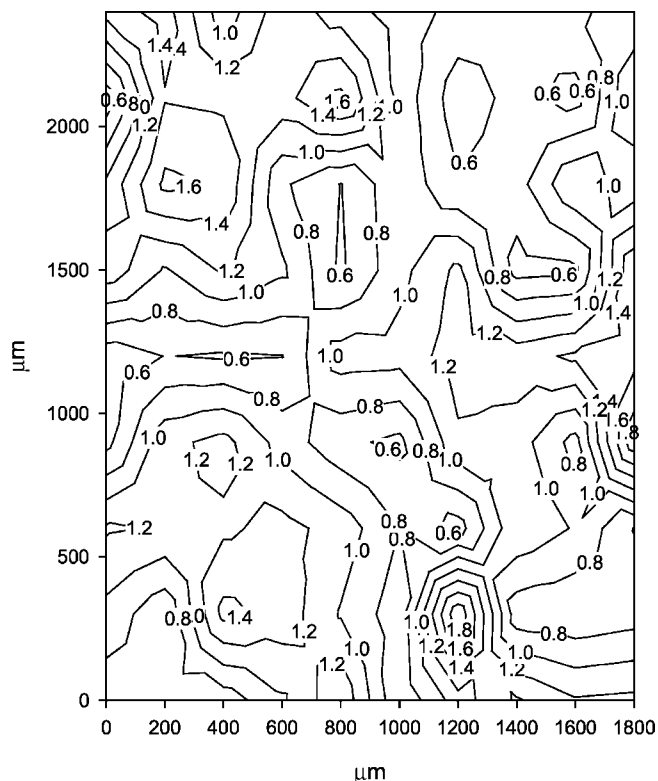


Fig. 5. Spatial distribution of the copper concentration in NR sheep liver, expressed in mg copper/kg of fresh weight, generated by raster scans.

these pattern in liver samples from animals with a normal metabolism. This technique could improve our knowledge of how trace elements are distributed in tissues on a micro- to millimeter scale. Because this technique is a multi-element method, it should be possible to identify similar zonations for other elements and find intrinsic relationships between different elements. This technique may potentially be useful for studying small samples from biopsies. For example, it can reveal where a metal-containing drug is accumulating, as in chemotherapy, or whether implants are releasing metals into the adjacent tissue. It may be possible to compare diseased organs with healthy organs and to identify differences in their trace element distributions. This could lead to further investigations into the cause of prion diseases, such as bovine spongiform encephalitis, Creutzfeldt-Jakob disease, or scrapie.

This project was supported by grants from the EPSRC (Grants GR/M91853/01, GR/R50837/01, and GR/R08049/01) and the Royal Society. A. K. thanks the University of Natal, Durban, for his sabbatical leave to the University of Aberdeen.

References

1. Watt F. Nuclear microscope analysis in Alzheimer's and Parkinson's disease: a review. *Cell Mol Bio* 1996;42:17–26.

2. Fuentealba IC, Haywood S, Trafford J. Evaluation of histochemical methods for the detection of copper overload in rat liver. *Liver* 1987;7:277–82.
3. Mesjasz-Przybylowicz J, Przybylowicz WJ. Micro-PIXE in plant science: present status and perspectives. *Nucl Instrum Methods B* 2002;189:470–81.
4. Todd PJ, Schaaf TG, Chaurand P, Caprioli RM. Organic ion imaging of biological tissue with secondary ion mass spectrometry and matrix-assisted laser desorption/ionization. *J Mass Spectrom* 2001;36:355–69.
5. Chandra S, Morrision GH. Imaging ion and molecular transport at subcellular resolution by secondary ion mass spectrometry. *Int J Mass Spectrom Ion Processes* 1995;143:161–76.
6. Iancu TC, Perl DP, Sternlieb I, Leshinsky E, Kolodny EH, Hsu A, et al. The application of laser microprobe mass analysis to the study of biological material. *Biometals* 1996;9:57–65.
7. Kupper H, Lombi E, Zhao FJ, Wieshammer G, McGrath SP. Cellular compartmentation of nickel in the hyperaccumulators *Alyssum lesbiacum*, *Alyssum bertolonii* and *Thlaspi goesingense*. *J Exp Bot* 2001;52:2291–300.
8. Ylanen HO, Ekholm C, Beliaev N, Karlsson KH, Aro HT. Comparison of three methods in evaluation of bone ingrowth into porous bioactive glass and titanium implants. *Key Eng Mat* 2000;192:613–6.
9. Centeno JA, Johnson FB. Microscopic identification of silicone in human breast tissues by infrared microspectroscopy and x-ray microanalysis. *Appl Spectrosc* 1993;47:341–5.
10. Mizuhira V, Hasegawa H, Notoya M. Microwave fixation and localization of calcium in synaptic terminals and muscular cells by electron probe X-ray microanalysis and electron energy-loss spectroscopy imaging. *Acta Histochem Cytochem* 1997;30:277–301.
11. Chaurand P, Caprioli RM. Direct profiling and imaging of peptides and proteins from mammalian cells and tissue sections by mass spectrometry. *Electrophoresis* 2002;23:3125–35.
12. Günther D, Jackson SE, Longerich HP. Laser ablation and arc/spark solid sample introduction into inductively coupled plasma mass spectrometers. *Spectrochim Acta* 1999;54B:381–409.
13. Feldmann J, Kindness A, Ek P. Laser ablation of soft tissue using a cryogenically cooled ablation cell. *J Anal At Spectrom* 2002;17:813–8.
14. Hoffmann E, Lüdke C, Skole J, Stephanowitz H, Ullrich E, Colditz D. Spatial determination of elements in green leaves of oak trees (*Quercus robur*) by laser ablation-ICP-MS. *Fresenius J Anal Chem* 2000;367:579–85.
15. Hansen HR, Hector BL, Feldmann J. A qualitative and quantitative evaluation of the seaweed diet of North Ronaldsay sheep. *Anim Feed Sci Technol* 2003;105:21–8.
16. Haywood S, Fuentealba IC, Kemp SJ, Trafford J. Copper toxicosis in the Bedlington terrier: a diagnostic dilemma. *J Small Anim Pract* 2001;42:181–5.
17. Gehardt R. Metabolic zonation of the liver—regulation and implications for liver-function. *Pharmacol Ther* 1992;53:275–354.
18. Kumaratilake JS, Howell JM. Histochemical study of the accumulation of copper in the liver of sheep. *Res Vet Sci* 1987;42:73–81.
19. Vogel A, Venugopalan. Mechanisms of pulsed laser ablation of biological tissues. *Chem Rev* 2003;103:577–644.